The superfluid transition of ^{4}He, a test case for finite-size scaling at a second-order phase transition

2001 J. Phys.: Condens. Matter 13 4871

(http://iopscience.iop.org/0953-8984/13/21/315)

INSTITUTE OF PHYSICS PUBLISHING JOURNAL OF PHYSICS: CONDENSED MATTER

J. Phys.: Condens. Matter **13** (2001) 4871–4889 www.iop.org/Journals/cm PII: S0953-8984(01)19773-0

The superfluid transition of ^{4}He, a test case for finite-size scaling at a second-order phase transition

Francis M Gasparini, Mark O Kimball and Kevin P Mooney

Department of Physics, University at Buffalo, SUNY, USA

Received 5 December 2000, in final form 23 March 2001

Abstract

The second-order phase transition of ^{4}He from a normal fluid to a superfluid is ideally suited for studies of critical behaviour. In particular, effects of confinement have been studied recently to verify theoretical predictions of correlation-length scaling and calculations of specific scaling functions. These predictions are summarized for the specific heat and the superfluid density. The method of achieving confinement is discussed, as well as the measuring technique. The specific heat and the superfluid density in planar confinement are examined. It is found that the specific heat scales well on the normal side, and just as well on the superfluid side until the region of the specific heat maximum is reached. Here deviations from scaling are seen. It is possible that this behaviour is associated with the specific crossover in two dimensions. The superfluid fraction, which has been measured for the same type of confinement in two different ways, does not scale. Results of a calculation for the superfluid density to assess the role of the inhomogeneity induced by the van der Waals attraction at the confining walls are presented.

(Some figures in this article are in colour only in the electronic version; see `www.iop.org`)

1. Introduction

The behaviour of a system near a second-order phase transition has been the subject of interest for a long time. One knows that the thermodynamic response is characterized by power laws. Thus, there are characteristic exponents which govern the singular behaviour as the transition is approached. One also knows that there are relationships among these exponents known as scaling laws. These limit the number of necessary exponents and amplitudes needed to describe a multitude of thermodynamic quantities. Further still, the behaviour of rather disparate physical systems, such as magnets and fluids, can be brought under the same umbrella via the concept of universality. This limits the number of classes one needs to consider to those which differ in spatial dimension, and in the vector character of the order parameter. This is a quantity such as the magnetization for a ferromagnet, or the difference between the liquid and gas density at the liquid–gas critical point, which vanish as one approaches the critical temperature T_c from below. Universality is also a concept which can be applied to the same physical system if there is a locus of second-order transitions along a line or a surface in

0953-8984/01/214871+19$30.00

thermodynamic space. Near T_c, fluctuations are manifest up to a length ξ, the correlation length, which diverges as T_c is approached from either side.

Liquid ^{4}He at saturated vapour pressure has a transition near $T_\lambda \cong 2.2$ K at which point the liquid goes from a normal state into a superfluid state. This transition is second order, and is marked by a near-divergence of the specific heat C_P, a vanishing of the superfluid density as T_λ is approached from below, and a divergent thermal conductivity as T_λ is approached from above [1]. The transition also extends over a range of pressures up to the freezing point near 30 bar, and over a range of ^{3}He–^{4}He concentrations. Thus, the locus of second-order transitions is a surface in the pressure–temperature–concentration space. This gives one a wide range of variables over which critical behaviour can be studied. One drawback in the case of helium is the fact that the order parameter is a wavefunction; thus there is no laboratory ordering field which one can manipulate. Hence, the susceptibility is not an accessible thermodynamic function. Within these limitations, the critical behaviour in helium is extremely well known and has yielded stringent checks of scaling and universality.

For the critical behaviour to be described by power laws as discussed above, it is required that the system be in the thermodynamic, or bulk limit. Even with the correlation length ξ diverging at the transition, this limit is not difficult to realize with typical laboratory samples. However, this is not always so. Even a large system might consist of small domains which can be comparable to ξ. Or by design, one might want to explore situations where a system is made finite deliberately to see how criticality is affected. This was first considered some time ago [2]. It was suggested that under appropriate conditions a finite system should be described by functions which can be calculated from the properties of the bulk system. No new critical exponents should emerge, but a scaling should be achieved with the variable ξ/L, where L is the smallest confining dimension [3]. This is not an easy prediction to verify experimentally, since it involves the realization of small samples with surfaces which are 'benign' to the ordering system. It also requires uniformity in the geometry of confinement, a point which is irrelevant in the thermodynamic limit. Finite systems are perforce geometry dependent. Thus, to study finite-size effects one must realize a series of confinements which are the same in all respects except in the small dimension L. The simplest examples of this are films with dimensions $L \times \infty \times \infty$, channels of $L \times L \times \infty$, and boxes, $L \times L \times L$. More complicated sample geometries in which a distribution of Ls is present are not suitable for studying correlation-length scaling. Also accompanying these *simple* geometries is the concept of dimensionality crossover to 2D, 1D, or 0D respectively depending on how many spatial directions are made small. This crossover might be particularly important in the case where in the lower dimension the system still exhibits its own criticality. In this case, the confined system will evolve in a continuous manner from bulk-like, to finite-size, and eventually cross over to a lower dimension as ξ grows with the approach to T_c. One should note that while ξ itself is renormalized by the confinement (it no longer diverges at T_c), the scaling of the thermodynamics is still done with the bulk ξ.

The superfluid transition of ^{4}He is well suited for studying finite-size effects. First and foremost a confining solid boundary terminates the order parameter without imposing an ordering field, or a field which constrains the system along a thermodynamic path where its response is not critical. Examples of this latter would be a fluid near the liquid–gas critical point in which density would be affected directly by the local pressure due to attraction of the walls. Another more subtle example might be a solid film formed on a substrate which constrains the film along a path in which the volume does not follow a path of constant pressure [4]. Another more obvious example is a magnetic boundary confining a magnetic film. With helium, confining walls do provide a local pressure gradient, and hence an inhomogeneity which breaks the expected ξ/L scaling. However, this effect is second order. Further, the

effect is highly local and can be estimated in a reasonable way in certain cases. Helium provides other advantages as well. Its critical behaviour in the bulk limit is very well known. In the case of the heat capacity for instance, measurements have been extended to a space environment where the effect of gravity is minimum and measurements have been made to within $t = |T/T_\lambda - 1| = 10^{-9}$ of the transition [5]. The superfluid properties offer some advantages in achieving confinement and controlling the measurements. Thermometry near 2 K can be done with high resolution and very stable platforms. In addition, there are theoretical calculations of specific scaling functions (beyond the ξ/L scaling *ansatz*) which are now available and apply to ^{4}He. More specifically they apply to XY systems, systems with two degrees of freedom in the order parameter.

There are at present no measurements of other systems near a second-order transition which have yielded results where overall scaling of a thermodynamic response can be done as in the case of ^{4}He near the superfluid transition. A review of earlier data for helium can be found in reference [6].

2. Experimental details

The first experimental requirement for studying finite-size effects in ^{4}He is the design and construction of an enclosure which will provide a uniform confinement. We have used a technique of direct wafer bonding to construct experimental cells which have exceptional homogeneity in the near-μm and sub-μm range [7, 8]. The concept is indicated schematically in figure 1. The design consists first of all of a silicon wafer which has a SiO_2 pattern formed lithographically. This pattern has an outer ring border (designed to seal the cell) and a series of SiO_2 posts (designed to space the wafers). A second wafer with a centre hole is bonded to this bottom wafer. This forms an enclosure of uniform small height L determined by the thickness of the oxide and effectively infinite (relative to ξ) lateral extent. The bonding of the two wafers involves a direct Si-to-SiO_2 room temperature contact bonding and subsequent annealing at higher temperatures. The structure of the cell can be monitored at various stages of assembly by using infrared imaging. In particular the spacing, if greater than 0.5 μm, can

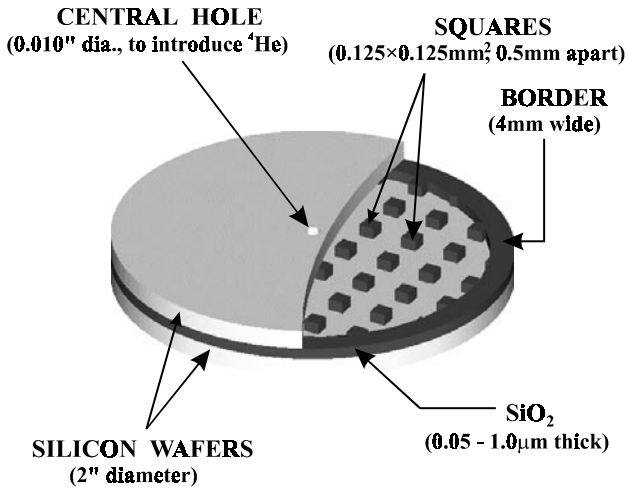

Figure 1. A cut-away view of a silicon cell to confine liquid helium. The smallest dimension is determined by the thickness of the oxide layer.

be measured interferometrically. It is typically uniform to better than 1% over the area of the cell. Cells with different Ls can be made to study effects of confinement. At present, cells in the range of 0.05 to 3.9 μm have been used in our work.

We have performed three types of measurement using these cells. One can stage them in such a way that the superfluid density can be determined by measuring the changes in mass loading of the cell as the helium becomes superfluid [9]. For this, the cell is made part of the moment of inertia of a high-Q torsional pendulum. Changes in the period of oscillation yield the superfluid fraction as the superfluid decouples from the motion of the confining walls. In another arrangement, one can measure the specific heat by imposing time-dependent temperature oscillations and examining the amplitude response [10]. The cell arrangement for this type of measurement is shown in figure 2. The cell is connected to a filling line which also provides a weak thermal link to an isothermal platform labelled S_1. Another weak thermal link is provided via copper wires to a second isothermal platform labelled S_2. This second link is used to ensure that the cell is colder than stage S_1. The cell has an evaporated film heater and two doped germanium resistors which are used as thermometers. When helium is condensed in the cell, most of it collects in the filling line immediately above the cell. This is bulk helium, and would give a much larger heat capacity signal than the helium confined in the cell. Thus, an adiabatic measurement of heat capacity is not possible. It would also not be possible *without* the helium in the filling line, since the requirement of good thermal isolation for such small sample would be very difficult to achieve. In an AC measurement, however, a frequency ω can be chosen such that only the confined helium responds while the bulk helium does not. Under certain conditions, one can write the amplitude of the detected temperature

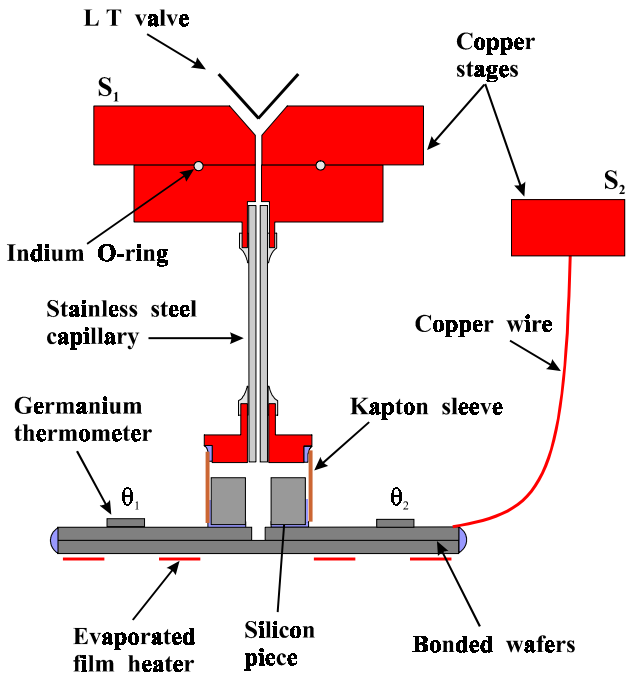

Figure 2. The experimental cell is staged at low temperature as indicated above. The connection to the helium filling line is via a stress-relief arrangement to prevent shattering of the silicon. Two thermometers provide temperature regulation and ac temperature read-out. Two isothermal stages define the isothermal environment.

oscillations T_{ac} as [10]

$$T_{ac} = \frac{Q_0}{2\omega C} f(\omega) g(\omega) \tag{1}$$

where Q_0 is the amplitude of the power applied to the heater, C is the desired heat capacity, and the functions f and g describe the rest of the frequency response. The first function describes principally a process whereby at low frequency T_{ac} is reduced due to heat losses to stage S_2; and, at higher frequencies, T_{ac} is reduced principally due to finite thermometer relaxation time [11]. The second function describes possible lateral temperature inhomogeneities over the surface of the cell [10]. This equation can be used to obtain both the heat capacity of the empty cell (30–60 μJ K^{-1} near 2 K) and the cell full of helium.

The arrangement of the cell shown in figure 2 can also be used to obtain the superfluid fraction. Below the transition, the superfluid will move readily in response to a chemical potential difference. Thus, if the cell becomes momentarily hotter than the filling line, superfluid will move into the cell from the filling line. This will increase the pressure, thereby providing a restoring force. We have called this adiabatic fountain resonance, AFR [12]. This mechanism has a characteristic resonance frequency ω_R given by

$$\omega_R^2 = \left(\frac{\rho_s}{\rho}\right) \frac{g}{\rho K} (1 + \gamma) \tag{2}$$

where ρ_s/ρ is the superfluid fraction, g is a geometric factor for the cell, K is the isothermal compressibility, and γ is a thermodynamic term which is typically about 0.02. This resonance, while useful in obtaining ρ_s/ρ, can actually interfere with the determination of the specific heat if ω_R is sufficiently close to the frequency at which the heat capacity is measured. On the other hand, if these frequencies are sufficiently separated, one can get two independent thermodynamic properties at the same time.

In figure 2 two thermometers are shown on the cell. We use one thermometer to regulate the *average temperature* of the cell. This can be done to within about 10^{-7} K. The other thermometer is DC biased and is used to detect the AC temperature oscillations. This can be done to better than 5×10^{-8} K by averaging the signal over several minutes.

The bulk helium which collects in the filling line performs two functions. It gives the important benchmark of T_λ, relative to which the scaling will be done, and provides a thermal ballast which is useful is stabilizing the average temperature of the cell.

3. Correlation-length scaling

A sketch of the specific heat of bulk helium and confined helium is shown in figure 3. One can use this to introduce various features of finite-size scaling. The specific heat of the bulk system, C_∞ has a singularity at T_λ. The confined system, on the other hand, has a rounded specific heat with maximum shifted to a lower temperature T_m. One expects that [2]

$$1 - T_m/T_\lambda = t_m = a_0 L^{1/\nu} \tag{3}$$

where ν is the exponent of the correlation length, 0.6705 [13, 14] for helium. This shift equation, as well as equivalent equations which focus on a particular points in $C(t, L)$ and how they vary with L, are all part of more general scaling equations which describe the overall 'missing signal' between $C_\infty(t)$ and $C(t, L)$. These can be written in such a way as to make most direct contact with theoretical calculations of the scaling functions [15, 16]:

$$[C(t, \infty) - C(t, L)]t^\alpha = \Delta C\, t^\alpha = (x)^\alpha f_2(x) = g_2(x) \tag{4}$$

$$[C(t, L) - C(t_0, \infty)]L^{-\alpha/\nu} = f_1(x) \tag{5}$$

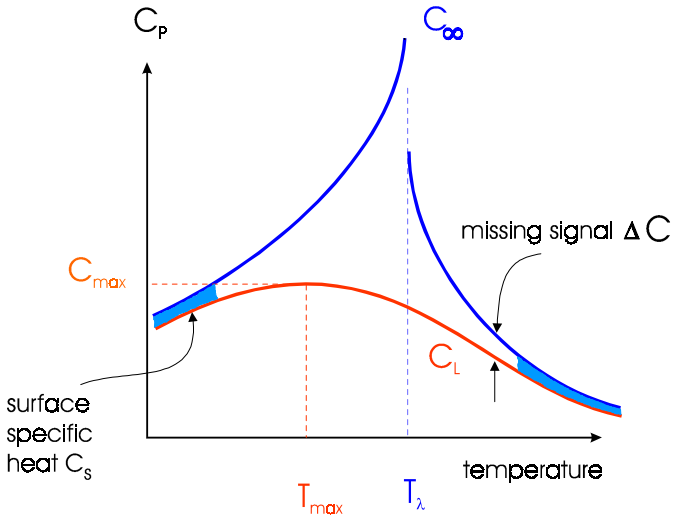

Figure 3. A sketch of the specific heat near the superfluid transition for a bulk sample, C_∞, and a sample confined to a small dimension L, C_L. Various features of the difference between the heat capacities can be described by scaling relations. See the text.

where $x = tL^{1/\nu}$ and α is the exponent of the specific heat, -0.0115 for helium [14, 17]. One can see that equation (3) can be obtained from (5) by setting the derivative of $C(t, L) = 0$. Similarly one can obtain an equation for $C_{max} = C(t_m, L)$:

$$C(t_m, L) = C(t_0, \infty) + f_1(x_m)L^{\alpha/\nu} \tag{6}$$

or for the value of the confined specific heat at $t = 0$:

$$C(0, L) = C(0, \infty) - f_1(0)L^{\alpha/\nu}. \tag{7}$$

In equations (5), (6), t_0 is the reduced temperature at which $\xi = L$. The two scaling functions $f_1(x)$ and $f_2(x)$ are related to each other [18]. Thus, if the data scale with one equation they will scale with the other. However, these two equations bring out different features of the data and are subject to different systematic errors in the analysis. For instance, for equation (4) one needs the detailed temperature dependence of $C(t, \infty)$, while for equation (5) one needs only the value at which the bulk correlation length is equal to L.

The qualitative behaviour of the superfluid density is shown in figure 4. Again, as in the case of the specific heat, one can say that the confinement decreases the superfluid fraction, and in particular causes it to vanish at a temperature below T_λ. Thus there is a missing signal which should be described by a scaling function. This can be written as [2, 19]

$$1 - \frac{\rho_s/\rho}{(\rho_s/\rho)_{bulk}} = f(tL^{1/\nu}). \tag{8}$$

Also indicated in figure 4 is a region labelled crossover. This is meant to indicate that, for instance for a film geometry, one should crossover into 2D; hence one should expect a discontinuity in the superfluid fraction very close to T_c [20]. This crossover should also take place in the specific heat but it was not indicated in figure 3. For the specific heat there is no particular structure expected (or observed) at T_c; in fact the specific heat maximum itself is not the location of T_c. This is expected to be at somewhat lower temperature [21], as has indeed been observed for thin films [22], and for the present data [23].

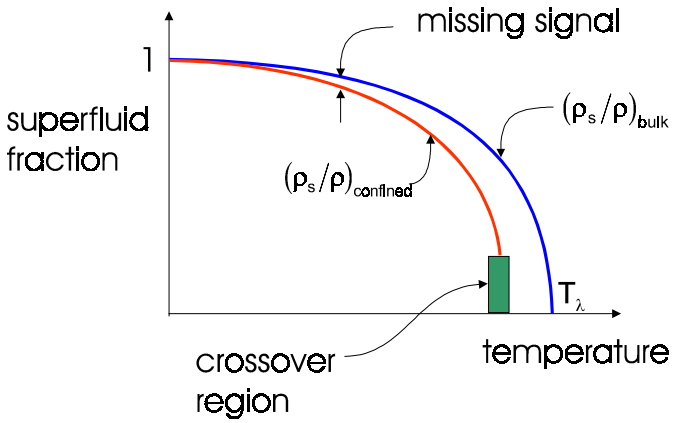

Figure 4. Behaviour of the superfluid density for confined and bulk helium. As for the specific heat, there is a missing signal which is described by a scaling function. The behaviour of the superfluid fraction in the crossover region depends on the lower dimension.

There is another way of looking at the effect of confinement, that is via surface properties (note that strictly surface properties independent of L can also be defined for an infinite system). This idea is applicable in the limit where $\xi \ll L$, but effects of confinements to a finite L are still observed. In this limit, one can break up the total free energy F into a bulk free energy per atom f_B and surface free energy per atom f_S [24]:

$$F \cong N f_B + N_S f_S. \tag{9}$$

The ratio N_S/N is the surface-to-volume ratio which for a film of thickness L is $2/L$. If one assumes that the bulk and surface specific heats are described by power laws with exponents α and α_S respectively, one can show that [25]

$$C(t,\infty) - C(t,L) = -\frac{2A_S}{L\alpha_S} t^{-\alpha_S}. \tag{10}$$

Thus, by comparing this with the expected scaling, equation (4), one can see that the surface exponent must be $\alpha_S = \alpha + \nu$. The amplitude of the surface specific heat A_S must be negative, and has recently been calculated [26]. In this limit, as can be seen from equation (10), the scaling function g_2 (see equation (4)) is pure power law with exponent ν.

4. Data and analysis

4.1. Specific heat

The data for helium confined in the planar geometry of the experimental cells described earlier are shown in figure 5 for $T > T_\lambda$ [18, 27]. Here data for six different confinements are plotted on a semilog scale as a function of the distance from T_λ. The qualitative behaviours of these data are as expected. For large values of t, or better, for values of t where $\xi \ll L$ (which occurs at different t for different L), the specific heats merge onto the behaviour of the specific heat in the thermodynamic limit. This is the solid line, which represents the combined measurements from many investigators [17][1]. Then, as one follows the confined data to smaller values of t, one by one the data for various Ls 'roll off' to a constant. This is the value $C(0, L)$ which

[1] An analysis of data from several investigators to yield a function useful over a broad range of t is carried out in reference [27].

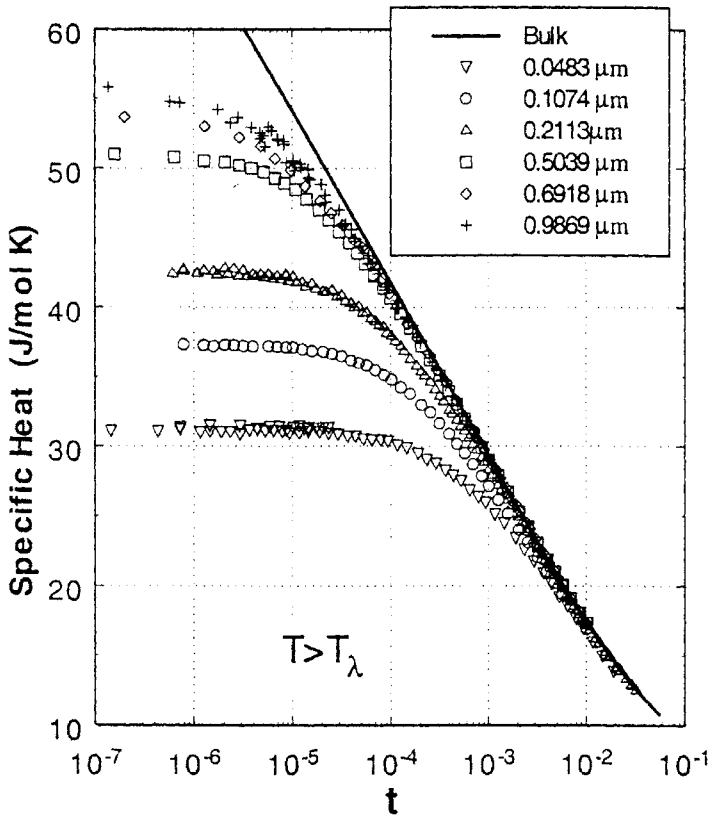

Figure 5. The specific heat for $T > T_\lambda$ for six different confinements.

is the point at which $C(t, L)$ crosses T_λ; see figure 3. These data should collapse when the difference between $C(t, \infty)$ and $C(t, L)$ is plotted according to equation (4). This scaling plot is shown in figure 6. This is a log–log plot of all these data. The first observation is *that all these data collapse on a universal locus with no systematics associated with the different Ls*. One can also add to these results data at 57 μm confinement given by Lipa *et al* [28] which also agree with these results.

The overall behaviour of the scaling locus is that for large values of the scaling variable this is described by the surface specific heat; see figure 3 and equation (10). The dashed line in this region of the data is the theoretical result of Mohr and Dohm for the amplitude A_S [26]. This calculation involves no adjustable parameters and only bulk properties. The agreement with the experimental results is excellent. See reference [18] for further discussion on this, and the role of dimensionality crossover. The surface specific heat description must fail as the scaling variable becomes smaller; one sees this as a deviation of the data from the straight line in figure 6. For very small values of $tL^{1/\nu}$ the curvature in the data is a reflection of the behaviour of $C(t, \infty)$. That is, as the confined system's specific heat rolls off to a constant, the dominant temperature dependence is that of the bulk specific heat. The fact that the data collapse in this region is still significant, since this depends of the measured value of $C(0, L)$. An empirical function which describes the full range of the scaling locus was obtained by Mehta *et al* [27]. The theoretical scaling function [29] which should describe the *full range of scaling* tends to fall below the data for small values of the scaling variable [18, 27]. This reflects

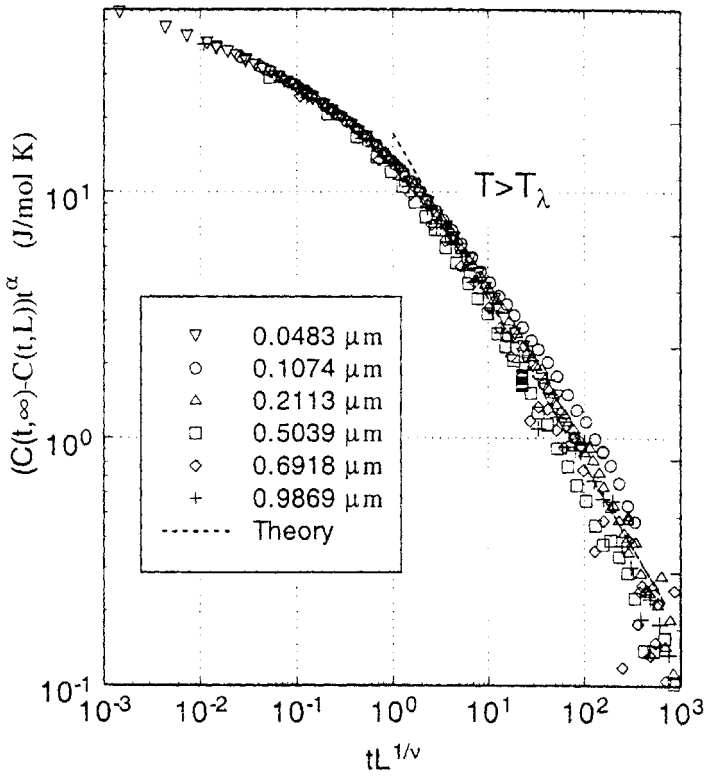

Figure 6. A scaling plot for the specific heat in the region $T > T_\lambda$.

an underestimate of the effect of confinement. This is also consistent with calculations which yield $C(0, L)$: these also yield larger values than what is obtained experimentally; see below.

We also note that a careful look at the region where the concept of a surface-plus-bulk properties applies shows that it extends to a value of about 9 in the scaling variable (note L is in Å). This translates into a ratio of $\xi(t, \infty)/L \sim 0.35$, which is surprisingly large. However, one should recall that the correlation length itself is renormalized due to confinement. We calculate that this ratio is closer to 0.2 if one takes a reasonable estimate for $\xi(t, L)/L$.

The data for $T < T_\lambda$ are shown in figure 7. Here a very similar behaviour for large values of t is seen as for $T > T_\lambda$, i.e. the data merge onto the solid line representing the bulk system. Not all of the data are continued to this limit because in some cases the onset of AFR distorts the heat capacity signal [23]. One can see in figure 7 that the specific heat maximum moves progressively further from T_λ as L is decreased and as equation (3) would indicate. The scaling of these data according to equation (4) is shown in figure 8. For clarity, only three sets of data are plotted here. See references [18, 27] for more comprehensive plots. One can see from figure 8 that the scaling for $T < T_\lambda$ is more complicated than for $T > T_\lambda$. First of all, there are no reliable theoretical calculations of the function $f_2(x)$ in the region of the specific heat maximum (the minimum in figure 8) with which the data can be compared. Even the surface specific heat calculation, which works so well for $T > T_\lambda$, does not work at all for $T < T_\lambda$ [26]. For small values of $tL^{1/\nu}$ in figure 8, one can see that there is as *good a scaling of these data as there is for* $T > T_\lambda$. This holds until the region of the minimum is reached. Significantly, the region of good collapse corresponds to the region where the confined system is still *normal*.

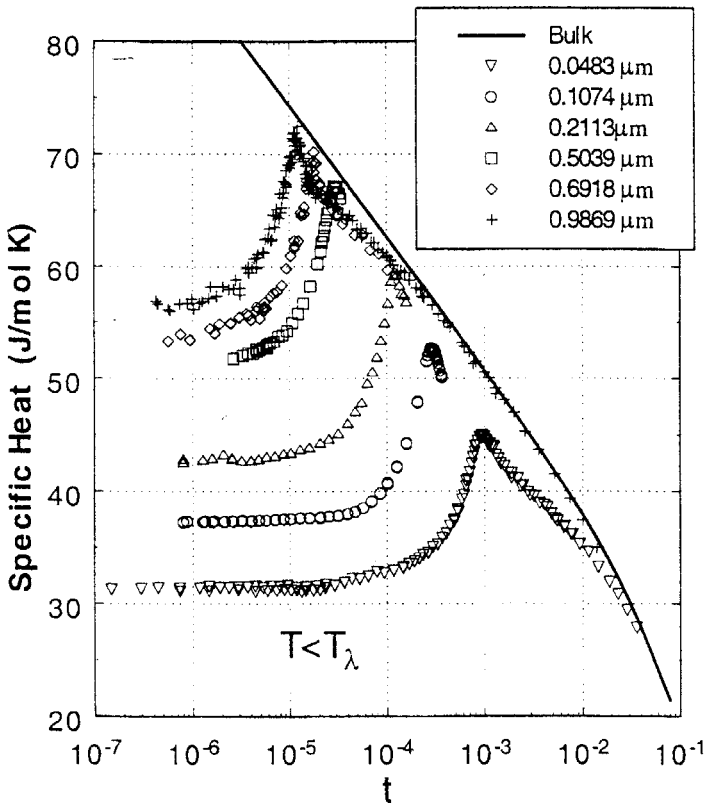

Figure 7. The specific heat for $T < T_\lambda$ for six different confinements.

The superfluid transition does not take place in these data until $tL^{1/\nu} \approx 12$, i.e. slightly to the right (the cold side) of the minimum in this figure. In the region of the minimum the data at smaller confinement lie higher than the data for larger confinement. This *lack of scaling* continues for larger values of $tL^{1/\nu}$—all in the *superfluid* region of the confined film.

We have suggested that the above behaviour is related to the 2D crossover of the confined films [18, 27]. In 2D, for an XY system, the maximum of the specific heat is not the location of the transition, but rather this occurs below the maximum. This is as observed experimentally in these data and for much thinner films as well [22]. The lack of scaling could be due to the fact that in 2D the specific heat is not universal [21]. This is reinforced by the observation that older data, taken with confinement in a cylindrical geometry (1D crossover) [15], do not show this behaviour [27]. However, this conclusion is based on measurements in which the confinement was certainly not as homogeneous as in the present experiments, and, just as important, it only covered reliably confinements over a range of a factor 2.5. The data in figure 5, 6 range over a factor of 20 in L. It is also interesting to note that data for the superfluid fraction in 2D confinement also do not scale. See below. Clearly, new measurements for 1D and for 0D crossover (for which none exist at present) would be necessary to clarify whether the lack of scaling comes with the onset of a non-zero order parameter, or is a reflection of 2D crossover.

In figure 9 are shown the data for $C(0, L)$ as function of confinement size. Unlike the previous scaling plots this plot does not rely on values of the bulk specific heat. $C(0, L)$ is measured directly. One can see that data for helium confined between silicon wafers, including

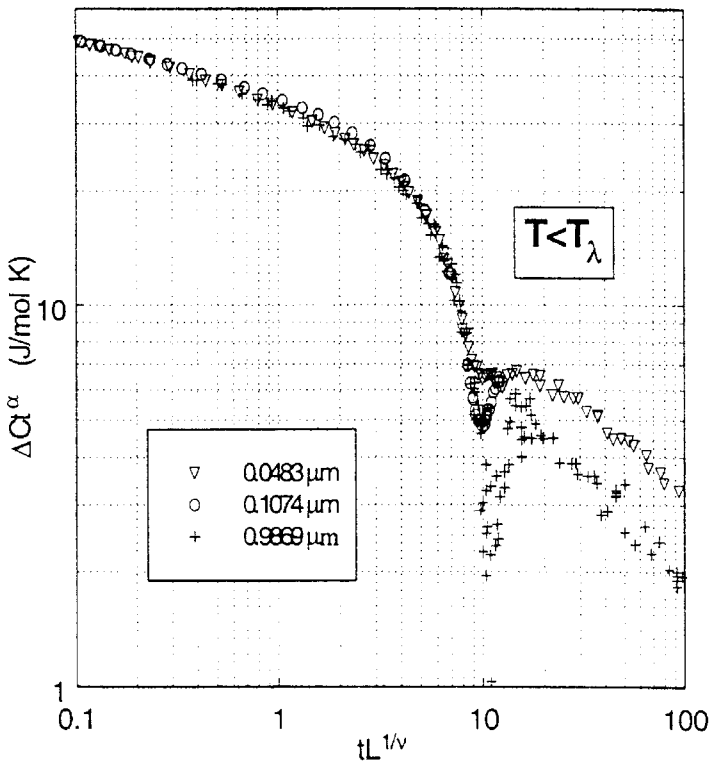

Figure 8. A scaling plot for the specific heat in the region $T < T_\lambda$.

the point at 57 μm from Lipa *et al* [28], as well as data for unsaturated films [15], all fall very nicely on a curve described by equation (7). The theory curve [30] lies slightly above these data. The calculation of reference [31, 32] lies much above the data. This indicates an underestimate in the theories of the effects of confinement. It is somewhat surprising that the data for unsaturated films (different boundary conditions, one solid surface, and a liquid–vapour interface) would fall in with data which represent confinement by two solid surfaces. This is surprising, as well, given the fact that the unsaturated films have thickness below 55 Å, a value one might consider too small to verify scaling effects. All of these facts suggest that this type of scaling (i.e. single-point scaling of $C(0, L)$ or C_{max} or $T_\lambda - T_{max}$ is not really very sensitive to some of the subtleties of confinement. Note in this regard that the position, i.e. shift of the specific heat maximum, also scales very well [27]; however, the value of the maximum as discussed in relation to figure 8 does not. See reference [18] for further analysis using the scaling function $f_1(x)$, and, in particular, for systematics associated with C_{max}.

4.2. Superfluid fraction

The superfluid density of helium confined within the silicon cells was measured in two different ways: with a torsional oscillator [9], and by making use of the adiabatic fountain resonance and equation (2) [12, 33]. Each method has some advantages and some disadvantages. With the torsional oscillator, a technique pioneered by Bishop and Reppy to study near monolayer films of helium [34], one looks for changes in the period of oscillation due to changes in mass

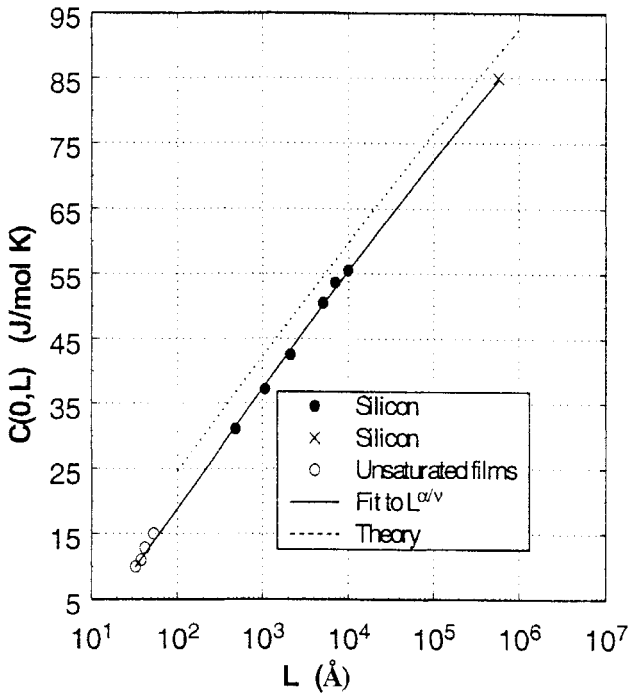

Figure 9. The scaling of the specific heat at $t = 0$, $C(0, L)$.

loading as the superfluid density varies. The helium, however, represents a small fraction of the total moment of inertia, a part in 10^4 to 10^5 depending on the design and sample. Thus, to resolve small changes in ρ_s one has to resolve the period of oscillation to better than a part in 10^8. This can be done. Ideally one should achieve a part in 10^9 or better. A strong advantage of this technique is that one can follow the changes in ρ_s through the transition without loss of signal.

In the case of AFR, the resonance determines the superfluid fraction directly, apart from a normalization of the magnitude to take care of certain geometric terms which are not well known. Thus, there is no large 'background' to worry about. However, the resonance becomes seriously damped as the transition is approached. An example of this is shown in figures 10, 11. Here are plotted the amplitude of the temperature response and the phase shift of the detected signal relative to the drive signal at the heater. Note in these figures that the temperature excursions measured are quite small (see the vertical bars in figures 10, 11). From either the temperature or phase signals one can get ω_R and other parameters of the resonance. For figure 10 the temperature is $t = 0.01$ while for figure 11, $t = 0.0013$. The difference between these data is striking. The increase in dissipation as t becomes small is manifest in the increase in the resonance linewidth. It was recently shown, in the case of ^{3}He–^{4}He mixtures, that the dissipation can be scaled with ξ, but the actual scaling locus is reflective of the growth of the 2D correlation length [33].

Dissipation is a characteristic of the 2D transition in which vortices play a central role [35]. However, it is also a problem in other geometries when a resonance involves confined helium [36]. Because of these effects, the resonance vanishes before the superfluid fraction does. This was first observed in third sound which is a resonance mode in very thin helium films [37]. The net result is that one cannot establish the behaviour of ρ_s very close to the

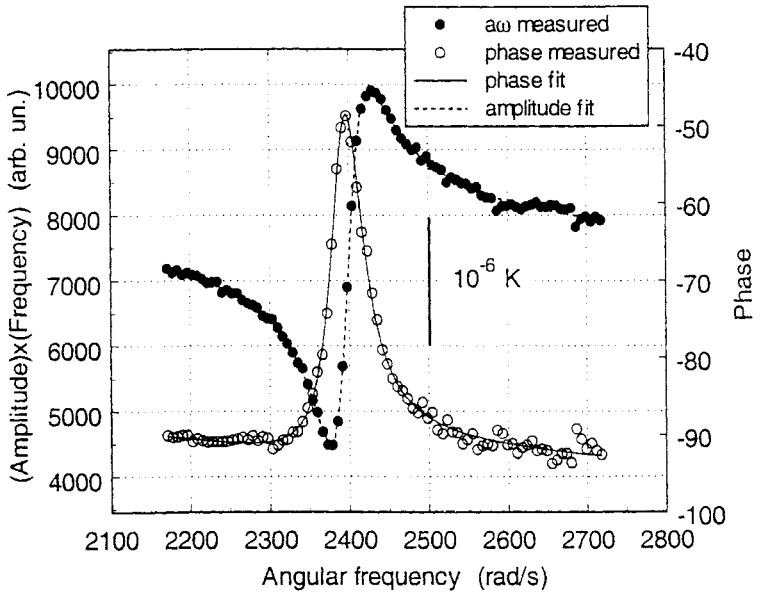

Figure 10. The resonance signal at $t = 0.0109$. Both amplitude and phase are well defined at this temperature. The lines through the respective data are fitted to theoretical functions describing the resonance.

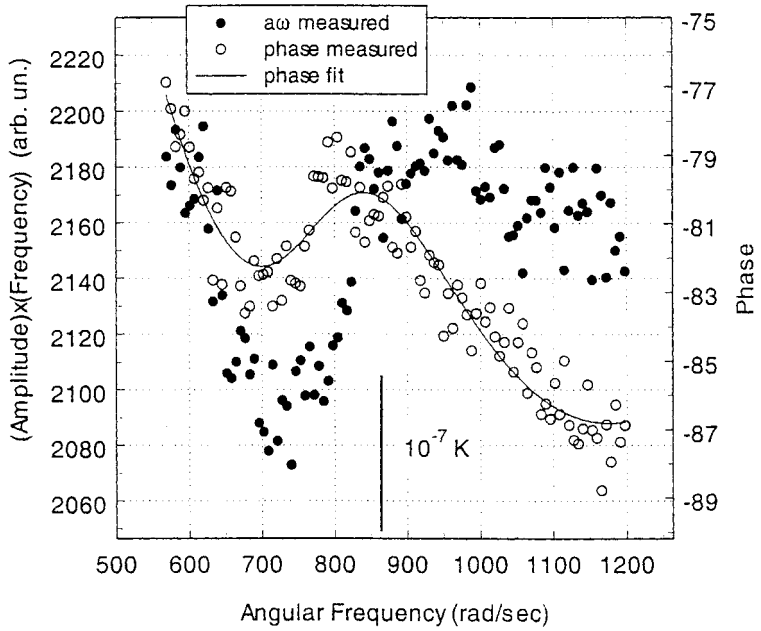

Figure 11. The resonance signal at the limit of resolution $t = 0.001\,29$. The solid line through the phase data is a fit to a theoretical function which describes the resonance.

transition. In the AFR with the silicon cells there is also dissipation as the confined helium communicates with the bulk helium in the filling line. In the design of some of our cells we

actually modified the region immediately below the central filling hole (see figure 2) to damp out the AFR completely. We did this because our primary interest was in the heat capacity, and the resonance often distorted these data which were taken at a fixed ω which would eventually overlap with the resonance on the superfluid side. The net result of this is that there are reliable AFR data for only two of the cells in which heat capacity data were also measured. For the torsional oscillator (TO) the data available are those of Rhee *et al* [9]. Altogether these data span a range of confinement of a factor of about 80.

Data for the superfluid fraction are shown in figure 12. The value at which, ideally, the data should have a discontinuous jump to 0 [20] is indicated by the short horizontal lines. One can see that the AFR data (circles and plus signs) are close to this limit. On the other hand, the TO data run continuously through this limit. The expected discontinuous jumps can only be realized in the DC limit and are rounded off at a finite frequency. The dashed line through the data is the behaviour of ρ_s/ρ in the thermodynamic limit [38]. The data at 0.0483 μm are represented by a dot and an open circle. This indicates independent results from either the phase data or the temperature amplitude data (see figures 10, 11). To scale all of these data according to equation (8), one needs to ratio the measured ρ_s/ρ to the bulk value, and plot this as a function of the scaling variable. This is shown in figure 13.

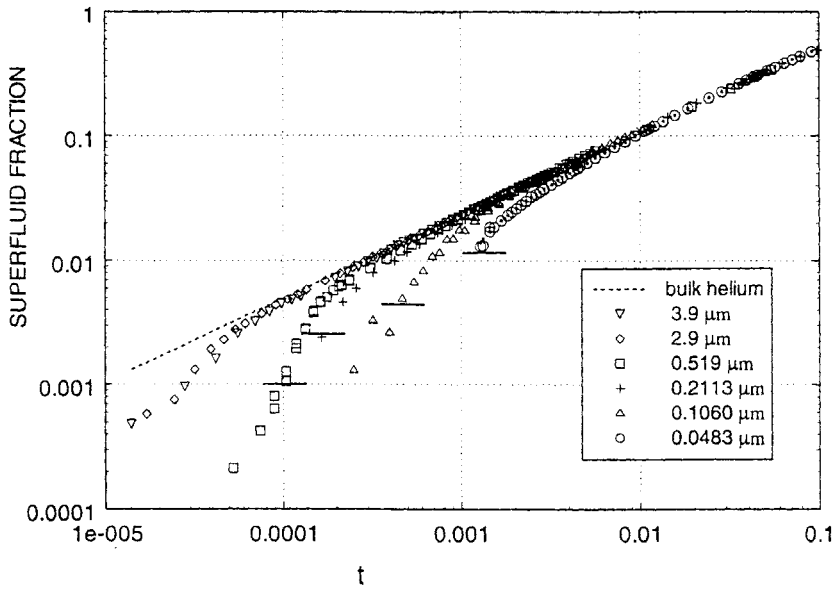

Figure 12. The superfluid fraction for six different planar confinements. Two different techniques were used to obtain these data. See the text.

It seems clear from figure 13 that *the superfluid density data do not collapse onto a universal curve*. They do not scale. There is a systematic trend in the data whereby the smaller confinements lie progressively to the left of the larger confinements. This lack of data collapse should be contrasted to figures 6 and 8 for the specific heat. The theoretical scaling function calculated from field theory is shown as the solid line on this graph [29]. The dashed curve will be discussed below. There are also results for the scaling function from numerical simulations of the 2D XY model [39]. Interestingly, these numerical simulations do not yield a collapse of the calculated data unless one adds a constant length scale to each L for which the simulation is done. This yields a universal function, but is contrary to the expectations of correlation-length

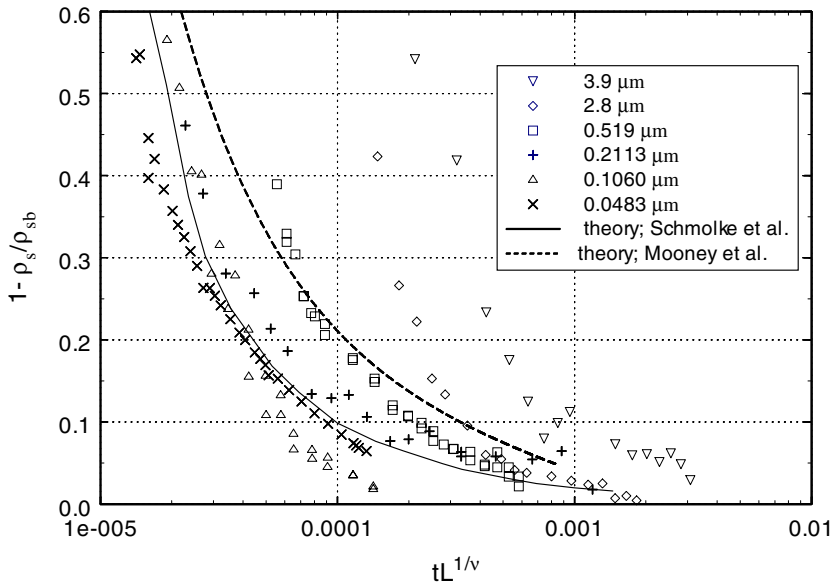

Figure 13. Data for the superfluid density plotted according to equation (8). The × and + symbols are for AFR data; the remaining symbols refer to TO data. For the theory curves, see the text.

scaling. Whether the problem with the lack of scaling with the experimental data is the same as with the numerical simulation is not clear. Adding a length scale to the experimental data has been tried, but what is required according to reference [39] is 0.145 μm, for an approximate collapse of the data. This seems quite a large length whose physical significance is unclear. Further, it seems quite arbitrary, given that the specific heat requires no such length scale. It is interesting to note, as remarked before, that the specific heat itself *near the maximum and on the superfluid side* does not scale as well. It was suggested earlier that the lack of scaling might be associated with the 2D crossover. It would be desirable to have ρ_s/ρ data for other crossover dimensions, but none are available to test scaling in the same way as in figure 12. See reference [36] for data on ρ_s/ρ for helium confined in a cylindrical geometry.

There is another way to examine the ρ_s/ρ data which is analogous with the surface-specific model used earlier. In the same spirit, one can expand the scaling function in equation (8) to obtain $f(t/L^{1/\nu}) \sim t^{-\nu}/L$. This expression can be used even with data where the confinement is not uniform and cannot be scaled with a particular L. That is, the initial deviation from bulk behaviour in any confinement is due to the proximity of the superfluid to a surface and the fact that the order parameter has to vanish. A number of data were analysed this way by Gasparini and Rhee [6]. They found that the data did obey a power law in t, but the exponent was close to 1 rather than the expected 0.67. See table 4 in reference [6].

5. Role of the confining surface

The surface which confines the helium plays two roles: it terminates the order parameter leading to finite-size effects, and it also provides, via the van der Waals attraction, an inhomogeneity which disrupts correlation-length scaling. In helium this attraction may be viewed as providing a local pressure which affects the superfluid transition. The value of T_λ, and the amplitudes of both the specific heat and the superfluid fraction are functions of pressure. In the case of

the superfluid fraction, a phenomenological theory due to Ginzburg and Pitaevskii [40] and modified by Mamaladze [41] can be used to describe inhomogeneities in the superfluid. Much work with this theory has been done by Ginzburg and Sobyanin [42] who refer to it as ψ-theory. In this theory one has to solve a differential equation for ψ which can be written as [42]

$$\nabla^2\psi = \frac{3}{3+M}\{-1+(1-M)\psi^2+M\psi^4\}\psi \tag{11}$$

where the equation has been written in terms of dimensionless spatial variables $\boldsymbol{r}/\xi_\psi$, with $\xi_\psi = 2.174(T_\lambda - T)^{-2/3}$ K$^{2/3}$ Å, and $\psi = \rho_s(\boldsymbol{r})/\rho_{s\ bulk}$. M is a parameter in the theory which typically takes values between 0 and 1. It does not play a strong role in the effects to be investigated. Note that equation (11), written as indicated, guarantees that the value of $\rho_s(\boldsymbol{r})/\rho_{s\ bulk}$, which has to be averaged over the volume of confinement, will be in scaling form. Equation (11) allows one to introduce an external potential via its effect on T_λ:

$$T_\lambda = T_{\lambda_0} + \frac{\mathrm{d}T_\lambda}{\mathrm{d}\mu}V(r). \tag{12}$$

Specifically, one can introduce the van der Waals potential energy in the form $V(z) = -\theta/z^3$ where θ is characteristic of the helium–silicon interaction, and z is the distance from the surface. There are no attempts in such an approach to include density variations (due to the local pressure) and variations in ξ_ψ due to density.

The calculation of the scaling function for ρ_s (in the absence of $V(z)$), and for planar confinement is shown as the dashed line in figure 13 [43]. There is not much one can say about agreement or disagreement of the calculation with the data since the data do not collapse onto a universal locus. Although the ψ-theory result clearly differs from the field-theory calculation, and thus might not be considered as reliable, it gives us a way to calculate the effects of the van der Waals field, by examining *relative changes* due to $V(z)$. A calculation of the ratio $(\rho_s(\boldsymbol{r})/\rho_{s\ bulk})_{ave}$ for the confinement at 0.0483 μm and 0.9869 μm is shown in figure 14 [43]. Also on this plot is this ratio in the absence of $V(z)$. As expected, the effect of the van der Waals field is small for the larger confinement. This can also be seen from the inset in this figure where the difference between the superfluid density ratio without and with $V(z)$ is shown. For the smaller confinement one can see that $V(z)$ lowers the value of the superfluid ratio substantially. From the inset, one can see that overall the effect is small at large values of the scaling variable, and more visible as t decreases. This is reasonable, since for large t the superfluid fraction is large and the surface influence amounts to a small perturbation of this value. For small t the situation is reversed: the superfluid density is already small and the van der Waals field has a more visible effect; ultimately it drives ρ_s to zero at a temperature below where it would have vanished for $V(z) = 0$.

On the basis of this calculation one can conclude that if one were to correct the superfluid density data for this effect (note that the experimental data *include* the effect of $V(z)$ for all confinements), one would have to *increase* the superfluid fraction of the smaller confinements relative to the larger. *This would make the disagreement with scaling as shown in figure 13 even worse*. Thus, based on this, the disagreement with scaling does not have as a source the inhomogeneity introduced by the walls.

We do not see a way to calculate from ψ-theory effects of $V(z)$ on the specific heat.

6. Summary and remarks

The way a finite system reaches its thermodynamic limit is one of the fundamental problems in statistical mechanics. Near a second-order phase transition, confinement to a finite size has a more marked effect due to the growth of the correlation length. To study these effects

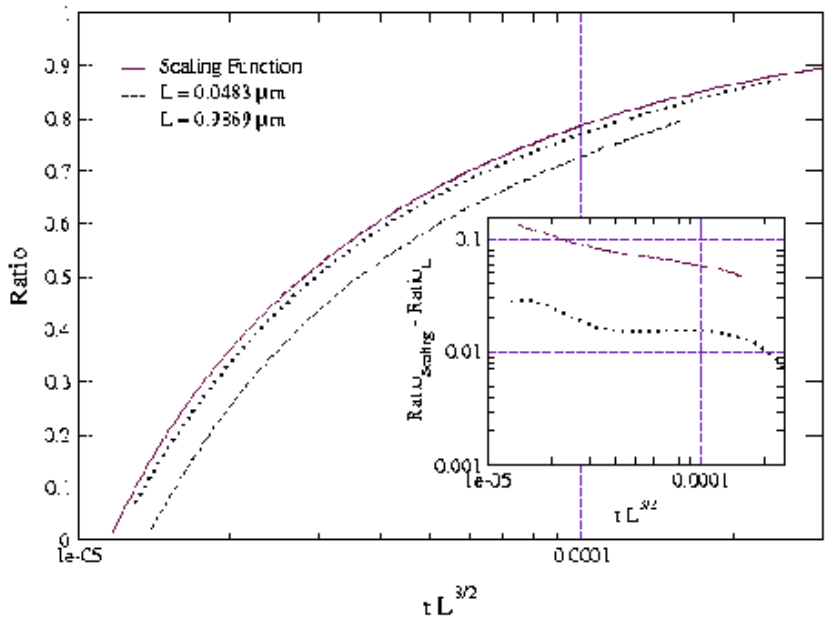

Figure 14. Ratio of confined to bulk superfluid fraction as a function of the scaling variable. The effects of the van der Waals potential are shown for two values of L. The inset emphasizes the difference between the solid line and the dashed lines [43].

one must recognize that they are dependent on the geometry of the sample. Thus, control of the homogeneity of confinement is just as important as the precision of the thermodynamic measurement. Simple geometries can be used so that one or more of the spatial dimensions are made small. In addition, one must recognize that for any given system the confining boundaries themselves might affect the order parameter in a critical way. The superfluid transition in ^{4}He is ideal for studying finite-size effects because of the nature of its order parameter, the detail in which the behaviour in the thermodynamic limit is known, and some advantages in thermometry and temperature control which can be realized at low temperatures. In addition, since the superfluid transition extends in the pressure–^{3}He-concentration plane, there exists the possibility of exploring the expected universal character of correlation-length scaling.

Measurements of the specific heat and superfluid density in a planar confinement between silicon wafers have yielded a number of results. The specific heat on the normal side of the transition scales very well with the exponent of the bulk correlation length. In addition the region which is describable by a surface specific heat agrees very well with theoretical calculations. Closer to the transition, one finds that the theoretical scaling function underestimates the effect of confinement. The region for $T < T_\lambda$ shows that the data scale well until one reaches the region of the specific heat maximum. Here the data separate systematically with an unexpected lack of scaling. It seems likely that this is a manifestation of the 2D crossover for these data. More measurements are needed for other confining geometries to confirm this conclusion.

Data for the superfluid fraction obtained using two different techniques do not scale. From examination of other data, which can be done using a limiting form of the scaling function, this seems to be a more global problem than in the case of the specific heat (at least judged on the basis of data available at present). It could turn out that the region where the order parameter

is not zero is the region where scaling fails. More data obtained under the controlled geometry of the planar silicon cell are necessary to reach a firmer conclusion. Certainly data for 1D crossover and 0D crossover would be desirable.

On the theory side, one must view the agreement with the surface specific heat calculation as very encouraging. More accurate calculations of the overall scaling function which would extend through the region of the maximum would be desirable. At the same time the calculation of the surface specific heat on the superfluid side remains a puzzle in its lack of agreement with the data. Perhaps this should not be worrisome, given that the data do not scale in this region. Numerical Monte Carlo calculations have been very helpful particularly in identifying the differences in dimensionality crossover for the specific heat [44]. These calculations also have revealed a lack of scaling for the superfluid fraction. It is not clear, however, whether this lack of scaling stems from the same root as in the experiments. Field-theory calculations of the superfluid density do not reveal any lack of scaling. However, recent results suggest possible lack of scaling, but in a region far from the transition [45].

In summary, much progress has been made in understanding finite-size scaling at the superfluid transition, but there are a number of unresolved puzzles and difficulties which await further experiments and theory for their resolution.

Acknowledgments

We are grateful to the National Science Foundation for continued support for our work, most recently through Grant DMR 9972287. We also acknowledge the Cornell Nanofabrication Facility for Grant 524-94.

References

[1] For a review of critical phenomena in helium see
Ahlers G 1978 *The Physics of Liquid and Solid Helium* part I, ed K H Bennemann and J B Ketterson (New York: Wiley)

[2] Fisher M E 1971 *Proc. 51st 'Enrico Fermi' Summer School on Critical Phenomena (Varenna, Italy)* ed M S Green (New York: Academic)
Fisher M E and Barber M N 1972 *Phys. Rev. Lett.* **28** 1516

[3] For a review of finite-size scaling see
Barber M N 1983 *Phase Transitions and Critical Phenomena* vol 8, ed C Domb and J L Lebowitz (New York: Academic)
Privman V 1990 *Finite Size Scaling and Numerical Simulations of Statistical Systems* ed V Privman (Singapore: World Scientific)
and for a collection of theoretical papers see
Cardy J L (ed) 1988 *Finite-Size Scaling* (Amsterdam: North-Holland)

[4] Lutz H, Scoboria P, Crow J E and Mihalisin T 1978 *Phys. Rev.* B **7** 3600

[5] Lipa J, Swanson D R, Nissen J A, Chui T C P and Israelsson U 1996 *Phys. Rev. Lett.* **76** 944

[6] Gasparini F M and Rhee I 1992 *Progress in Low Temperature Physics* vol 13, ed D F Brewer (New York: North-Holland)

[7] Rhee I, Bishop D J, Petrou A and Gasparini F M 1990 *Rev. Sci. Instrum.* **61** 1528

[8] Mehta S, Yu W Y, Petrou A, Lipa J, Bishop D and Gasparini F M 1996 *Czech. J. Phys.* **46** 133

[9] Rhee I, Gasparini F M and Bishop D J 1989 *Phys. Rev. Lett.* **63** 410

[10] Mehta S and Gasparini F M 1998 *J. Low Temp. Phys.* **110** 287

[11] Sullivan P F and Seidel G 1968 *Phys. Rev.* **173** 679

[12] Gasparini F M and Mehta S 1998 *J. Low Temp. Phys.* **110** 293

[13] The exponent ν is obtained from measurements of the superfluid density:
Goldner L S and Ahlers G 1992 *Phys. Rev.* B **45** 13 129
and see also
Goldner L S, Mulders N and Ahlers G 1993 *J. Low Temp. Phys.* **93** 131

Greywall D S and Ahlers G 1973 *Phys. Rev.* A **7** 2145
Ahlers G 1981 *Physica* B **107** 347
Marek D, Lipa J A and Philips D 1988 *Phys. Rev.* B **38** 4465
Swanson D R, Chui T C P and Lipa J A 1992 *Phys. Rev.* B **46** 9043
[14] For the latest theoretical calculation of ν and α see
Campostrini M, Pelissetto A, Rossi P and Vicari E 2000 *Phys. Rev.* B **61** 5905
[15] Equation (4) was first used in
Chen T-P and Gasparini F M 1978 *Phys. Rev. Lett.* **40** 331
[16] Equation (5) was proposed in
Schmolke R, Wacker A, Dohm V and Frank D 1990 *Physics* B **165+166** 575
[17] The exponent for the specific heat has been obtained in a number of experiments. The experiment in reference [5] explores the region closest to T_λ; others contribute in the temperature region further from the transition and on the normal side. A collective analysis to obtain a good global representation of the heat capacity was carried out in reference [27] using data from the following references:
Ahlers G 1971 *Phys. Rev.* A **3** 696
Gasparini F M and Moldover M 1975 *Phys. Rev.* B **12** 93
Chen T P 1978 *PhD Thesis* State University of New York at Buffalo, NY
Lipa J A and Chui T C P 1983 *Phys. Rev. Lett.* **51** 2291
[18] Kimball M O and Gasparini F M 2001 *J. Low Temp. Phys.* **121** 29
[19] Binder K and Hohenberg P C 1972 *Phys. Rev.* B **6** 3461
Binder K and Hohenberg P C 1974 *Phys. Rev.* B **9** 2194
[20] Nelson D R and Kosterlitz J M 1977 *Phys. Rev. Lett.* **39** 1201
[21] Berker A N and Nelson D R 1979 *Phys. Rev.* B **19** 2488
[22] Yu Y Y, Finotello D and Gasparini F M 1989 *Phys. Rev.* B **39** 6519
[23] Mehta S and Gasparini F M 1997 *Phys. Rev. Lett.* **78** 2596
[24] This formulation is used in a number of sources; the earliest we are aware of in the case of critical behaviour is
Fisher M E and Ferdinand A E 1967 *Phys. Rev. Lett.* **19** 169
but see also reviews in reference [3] for similar formulations for edges and corners.
[25] Gasparini F M, Chen T-P and Bhattacharyya B 1981 *Phys. Rev.* B **23** 5797
[26] Mohr U and Dohm V 2000 *Physica* B **284** 43
[27] Mehta S, Kimball M O and Gasparini F M 1999 *J. Low Temp Phys.* **114** 467
[28] Lipa J A, Swanson D R, Nissen J A, Geng Z K, Williamson P R, Stricker D A, Chui T C P, Israelsson U E and Larson M 2000 *Phys. Rev. Lett.* **84** 4894
[29] Schmolke R, Wacker A, Dohm V and Frank D 1990 *Physics* B **165+166** 575
and see also
Dohm V 1993 *Phys. Scr.* T **49** 46
[30] Sutter P and Dohm V 1993 *Physica* B **194+195** 613
[31] Krech M and Dietrich S 1991 *Phys. Rev. Lett.* **66** 345
[32] Krech M and Dietrich S 1992 *Phys. Rev.* A **46** 1886
[33] Kimball M O and Gasparini F M 2001 *Phys. Rev. Lett.* **86** 1558
[34] Bishop D J and Reppy J D 1978 *Phys. Rev. Lett.* **40** 1727
Bishop D J and Reppy J D 1980 *Phys. Rev.* B **22** 5171
[35] Ambegaokar V, Halperin B I, Nelson D R and Siggia E D 1980 *Phys. Rev.* B **21** 1806
[36] Brooks J S, Sabo B B, Schubert P C and Zimmermann W Jr 1979 *Phys. Rev.* B **19** 4524
[37] Rudnick I 1978 *Phys. Rev. Lett.* **40** 1454
[38] We used the data of Greywall and Ahlers:
Greywall D S and Ahlers G 1973 *Phys. Rev.* A **7** 2145
[39] Schultka N and Manousakis E 1996 *Czech. J. Phys.* **46** 451
[40] Ginzburg V L and Pitaevskii L P 1958 *Zh. Eksp. Teor. Fiz.* **34** 1240 (Engl. Transl. 1958 *Sov. Phys.–JETP* **7** 858)
[41] Mamaladze Yu G 1967 *Zh. Eksp. Teor. Fiz.* **52** 729 (Engl. Transl. 1967 *Sov. Phys.–JETP* **25** 479)
[42] Ginzburg V L and Sobyanin A A 1976 *Usp. Fiz. Nauk* **120** 153 (Engl. Transl. 1976 *Sov. Phys.–Usp.* **19** 773)
Sobyanin A A 1972 *Zh. Eksp. Teor. Fiz.* **63** 1780 (Engl. Transl. 1973 *Sov. Phys.–JETP* **36** 941)
Ginzburg V L and Sobyanin A A 1987 *Japan. J. Appl. Phys.* **26** 1785
Ginzburg V L and Sobyanin A A 1982 *J. Low Temp. Phys.* **49** 507
[43] Mooney K P and Gasparini F M 2001 to be published
[44] Schultka N and Manousakis E 1998 *J. Low Temp. Phys.* **111** 783
[45] Chen X S and Dohm V 1999 *Eur. Phys. J.* B **7** 183